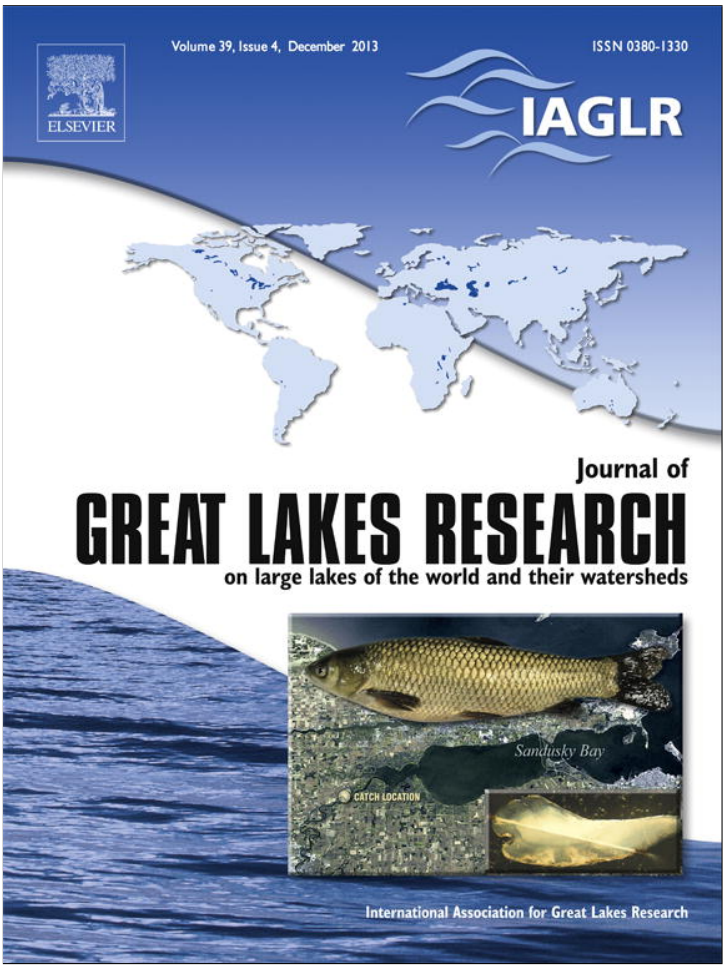

Journal of Great Lakes Research 39 (2013) 646–654

Contents lists available at ScienceDirect

Journal of Great Lakes Research

journal homepage: www.elsevier.com/locate/jglr

Mathematical modeling of bacteria–virus interactions in Lake Michigan incorporating phosphorus content

Audrey Béchette [a], Tom Stojsavljevic [b], Maxx Tessmer [a,b], John A. Berges [a], Gabriella A. Pinter [b], Erica B. Young [a,*]

[a] Department of Biological Sciences, University of Wisconsin — Milwaukee, 3209 N Maryland Ave, Milwaukee, WI 53211, USA
[b] Department of Mathematical Sciences, University of Wisconsin — Milwaukee, 3200 N Cramer Street, Milwaukee, WI 53211, USA

ARTICLE INFO

Article history:
Received 17 December 2012
Accepted 28 August 2013
Available online 7 October 2013

Communicated by William D. Taylor

Keywords:
Virus
Phytoplankton
Bacteria
Mathematical model
Phosphorus limitation
Cell quota

ABSTRACT

Viruses are ubiquitous in aquatic ecosystems and play a critical role in nutrient cycling because viral lysis of cells releases phosphorus, an essential and often limiting nutrient. Previous models have examined dynamics of bacterial and viral communities, but with limited analysis and without explicit consideration of nutrients. A recent model (Fuhrman et al., 2011; Math. Comp. Model. 53, 716-730) incorporated internal nutrient content of bacteria and viruses. In the present study, we modified and tested the model with data from natural planktonic communities from Lake Michigan. Replicate 20 L water samples (135 μm screened), were either untreated or enriched with 8 μM phosphate, and bacterial and viral abundance, chl *a* fluorescence, and phosphorus (total and dissolved inorganic) were monitored for two weeks. Fuhrman et al.'s model (modified to include phytoplankton) was applied to the data, fitting burst size, lytic latent period and virus decay rate. For enriched samples, model fits were good and parameters were consistent with measurements in other freshwater ecosystems. However, for unenriched samples, where nutrient concentrations approached detection limits, model fits were relatively poorer. The model predicted similar viral decay rates but higher burst sizes and longer latent period in phosphorus-limited versus enriched conditions, underlining the potential importance of nutrients in host–virus interactions. The model is likely to be most useful in meso- to eutrophic systems; requirements for future model development and parameter estimation for application to oligotrophic lakes are discussed.

Introduction

Viruses are abundant and ubiquitous in freshwater ecosystems and their roles in mediating trophic energy transfer in aquatic ecosystems have been recognized (Middelboe et al., 2008; Weinbauer et al., 2011). Attention has recently been paid to viruses as mediators in nutrient cycling (DeBruyn et al., 2004; Fuhrman, 1999). Infection and lysis of planktonic host cells can release nutrients into the water column for uptake by other organisms, effectively 'short-circuiting' grazer-driven nutrient recycling (DeBruyn et al., 2004; Gobler et al., 1997; Jacquet et al., 2010; Thomas et al., 2011); this has been demonstrated for the limiting nutrients including nitrogen and iron in marine systems (Gastrich et al., 2004; Gobler et al., 1997; Poorvin et al., 2004).

In freshwaters, including most of the upper Great Lakes, phosphorus (P) is typically the nutrient chronically limiting primary production by phytoplankton (Schindler, 1977), therefore characterizing the role of virus infection in P cycling is an essential component of understanding biogeochemical nutrient cycling in these freshwater ecosystems. Importantly, the factors driving virus–host dynamics in freshwaters may be distinct from those in marine ecosystems (Clasen et al., 2008; Wilhelm and Matteson, 2008). An understanding of the ecological significance of viruses in freshwater ecosystems requires an improved quantification of nutrient release by viruses in the context of nutrient limitation, but also a better grasp of community and population-level host–virus dynamics, including parameters such as burst size (number of intracellular lytic viruses per bacterium) and latent period (the time from virus infection to cell lysis).

The body of research on the role of viruses in nutrient cycling has been increasing, but mostly for marine systems (Jacquet et al., 2010). However, the small scale and rapid rate of viral infection and phytoplankton and bacterioplankton cell lysis, plus lack of knowledge about the specificity of virus–host interactions, mean that in situ measurements of transformation and fluxes of nutrients as a result of population-level viral processes are challenging. A powerful complementary approach to empirical study is the development of mathematical models to describe host–virus interactions (e.g., Beretta and Kuang, 1998; Gons, 1995; Gons et al., 2006; Middelboe, 2000). However, these models have typically not included the role of virus infection in nutrient release and cycling.

* Corresponding author. Tel.: +1 4142293257.
E-mail addresses: audrey@uwm.edu (A. Béchette), tgs@uwm.edu (T. Stojsavljevic), mtessmer@uwm.edu (M. Tessmer), berges@uwm.edu (J.A. Berges), gapinter@uwm.edu (G.A. Pinter), ebyoung@uwm.edu (E.B. Young).

0380-1330/$ – see front matter © 2013 International Association for Great Lakes Research. Published by Elsevier B.V. All rights reserved.
http://dx.doi.org/10.1016/j.jglr.2013.09.003

A model of aquatic host–virus dynamics developed recently by Fuhrman et al. (2011) combined existing models of bacteria and virus interactions (Beretta and Kuang, 1998; Gons, 1995; Gons et al., 2006; Middelboe, 2000) with models of nutrient uptake and cycling (Cunningham and Nisbet, 1983; Droop, 1974; Fu et al., 2005). Fuhrman et al. (2011) introduced a growth rate for the susceptible host which depends on the nutrient content of host cells (cell quota, Q, sensu Droop, 1974), addressing the need to consider nutrient limitation, which is common in many aquatic ecosystems. The Fuhrman et al. (2011) model forms the basis of the representation of virus–host dynamics in aquatic systems shown in Fig. 1. The model divides the bacterial host population into susceptible hosts, S, and infected hosts, I, which interact with free viruses, V, and free nutrient, N (representing phosphorus in this case for the typically P limited Great Lakes ecosystems). N_T represents the total nutrient in the system (free nutrient, plus nutrient contained in hosts and viruses as well as algae); this is measured total P. In order to fit the model, N_T is assumed to be constant allowing the differential equations (see below) to be solved. For purposes of the model, it is assumed that all free nutrient (dissolved P) is available to cells, and that all particulate P is contained in cells or viruses. Both susceptible and infected host cells take up free nutrient and incorporate it into their nutrient content, Q, used for growth. Susceptible hosts, S, can either become infected, I, or die at rate δ. Upon death, the cell's nutrient content, Q, is released into the environment. Although, in reality, not all cellular P released by viral lysis will be bio-available, the model assumes that Q is instantaneously available as free nutrient (N) (Fig. 1). Free virus, V, and the susceptible host, S, have an interaction following the law of mass action with susceptible host cell infection rate dependent upon K, the co-efficient of volumetric host–virus interaction (described by Fuhrman et al. (2011) as contact rate, and essentially the same as the contact rate estimated by Murray and Jackson, 1992). The length of time between host cell infection and lysis follows an exponential distribution with expected value 1/λ (where 1/λ is termed the latent period). Once an infected host cell lyses, b new viruses are released into the environment (where b is termed the burst size). Some of the nutrient stored inside the infected cell, I, is used to create new viruses; after host lysis, the rest enters the free nutrient pool, N. Thus, the basic equations of the model are:

$$dS/dt = \mu(Q)S - \delta S - KSV \quad (1)$$

$$dI/dt = KSV - \lambda I \quad (2)$$

$$dV/dt = -KSV + b\lambda I - dV \quad (3)$$

The essential equations that then link the bacterial and viral dynamics to free nutrient concentration are:

$$dQ/dt = \rho(N,Q) - \mu(Q)Q \quad (4)$$

$$\mu(Q) = \mu_{max}(1 - Q_{min}/Q) \quad (5)$$

$$\rho(N,Q) \equiv \rho(N) = \rho_{max}N(K_n + N)^{-1} \quad (6)$$

where μ(Q) is a growth function which follows Michaelis–Menten kinetics and ρ(N,Q) is a nutrient uptake function which follows a Monod kinetic. Additional symbols of model coefficients and their units are listed in Table 1.

Fuhrman et al. (2011) developed and analyzed their model mathematically, but did not test the model using experimental data, nor included nutrient uptake by phytoplankton. Their model also incorporated nutrient status of host cells into the model, but did not specifically analyze model predictions comparing nutrient replete versus nutrient limited conditions. The aim of the present study was to modify and test the Fuhrman et al. (2011) model using experimental data, comparing the model performance in carefully-controlled natural communities of viruses, bacteria and algae under either nutrient replete or nutrient depleted conditions. If the basic model proves workable, it can be integrated it into a broader ecosystem model. As such, we did not attempt to incorporate factors such as light and temperature in the model, nor did we add grazing terms for bacteria, or viruses. These factors were held constant for simulations or eliminated to the best of our ability. Because

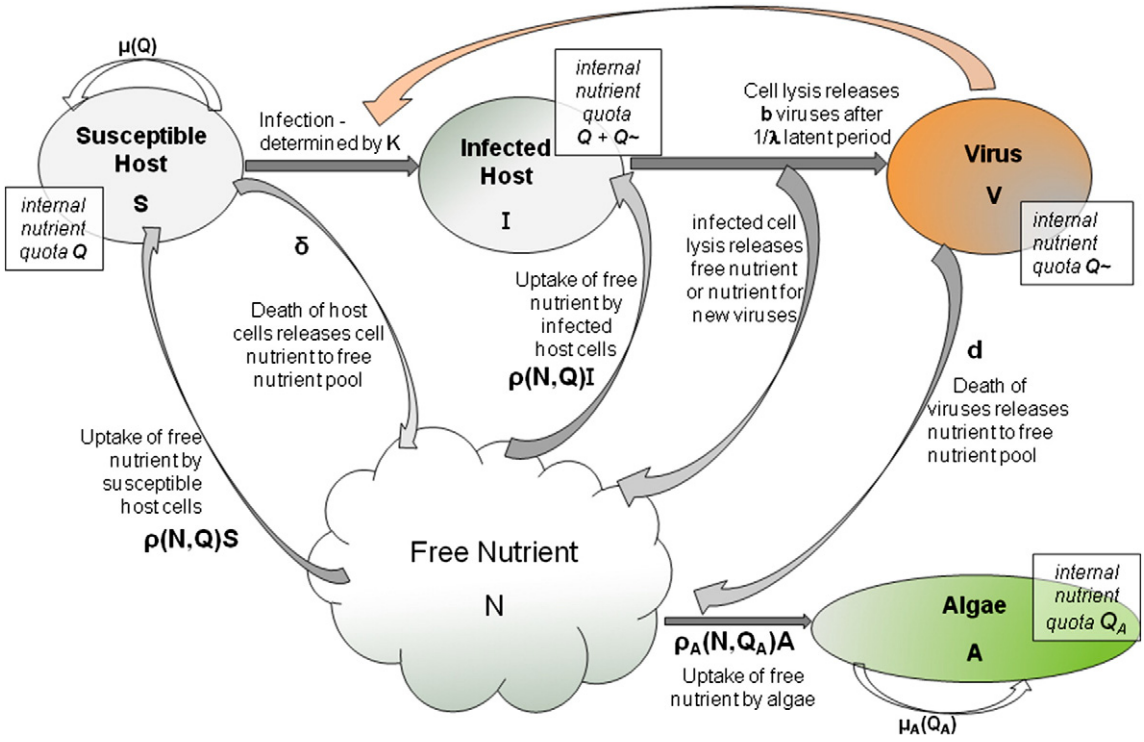

Fig. 1. Conceptualized nutrient flow in a lytic viral infection within freshwater ecosystems showing key variables and parameters used in the model (see also Table 1).

Table 1
Parameter values held constant and used in the model, with values derived from the literature, and explained in Fuhrman et al. (2011), for nutrients measured in each experimental carboy. Table 2 gives final optimized values of the parameters which were allowed to vary in the model (burst size, b, latent period, λ, and virus decay rate, d).

Parameter	Explanation	Values used in model simulation	Units	Reference
μ_{max}	Maximum growth rate of susceptible host	1.8	/d	Fuhrman et al. (2011)
δ	Death rate of the susceptible host	0.25	/d	Fuhrman et al. (2011)
K	Co-efficient of volumetric host–virus interaction[a]	1.03×10^{-11}	L/virus/d	Fuhrman et al. (2011)
Q_{min}	Minimum host cell P quota	0.0123	fmol	Fuhrman et al. (2011)
Q^-	Virus P quota	4.106×10^{-4}	fmol	Fuhrman et al. (2011)
K_n	Half saturation constant for P uptake by susceptible host	0.373×10^9	fmol/L	Fuhrman et al. (2011)
ρ_{max}	Maximum P uptake rate	0.0114	fmol/cell/d	Fuhrman et al. (2011)
N_T	Total nutrient	Control: 0.562×10^9 Enriched: 8.37×10^9	fmol/L	Calculated from experimental data
$\mu_{max\ A}$	Maximum growth rate of algae	0.5	/d	Schelske et al. (1974)
$Q_{min\ A}$	Minimum algal cell P quota	5	fmol	Smith and Kalff (1982)
$K_{n\ A}$	Half saturation constant for P uptake by algal cells	8.0×10^7	fmol/L	Smith and Kalff (1982)
$\rho_{max\ A}$	Maximum P uptake rate of algal cells	25	fmol/cell/d	Smith and Kalff (1982)

[a] Described by Fuhrman et al. (2011) as "contact rate".

phytoplankton accounted for the majority of nutrient uptake, it was necessary to add them to the basic model, added as a nutrient sink; recycling of nutrient taken up by algae was not included. We examined the dynamics of natural bacterial and virus communities, chlorophyll from phytoplankton, and free nutrient (P) over 14 days in water samples from Lake Michigan, either under phosphorus enrichment or untreated control conditions. The data collected were fit using a modified version of the Fuhrman et al. (2011) model and the model fit and resulting parameter estimates were assessed.

Methods

Sampling and cultures

Water samples were collected on July 6, 2010 from the *R/V Neeskay* at Fox Point, Lake Michigan (43° 11.670′ N, 87° 140.248′ W, 100 m deep) from 7.5 m depth using Niskin bottles. Samples were screened through Nitex mesh (with measured mesh opening of 135 μm), to remove larger grazers, transferred to four 20 L carboys and returned to the laboratory. Large phytoplankton are rare at the Fox Point station at this time of the year and previous work at the same site and time of year demonstrated that smaller 53 μm Nitex mesh excludes a maximum of 6% total chl *a* (Sandgren and Berges, unpublished). After 7 days of acclimation in low light, replicate carboys were enriched to ~8 μM phosphate, added as KH_2PO_4. The other two carboys served as unenriched controls. Carboys were maintained at 16 °C, with 64–90 μmol photons/m^2/s (16:8 light: dark cycle) and gently bubbled with filtered air. Experiments were monitored for 14 days after enrichment.

Determination of phosphorus pools

Triplicate samples were collected daily from each carboy for determination of soluble (molybdate) reactive phosphorus (SRP). SRP was determined on filtrates using the ammonium molybdate assay (Parsons et al., 1984), reading absorbance at 885 nm in a 10 cm pathlength cuvette. Total phosphorus (TP) was determined on samples from days 2–14 using a method based on potassium persulfate digestion (Menzel and Corwin, 1965); appropriate blanks and standards of KH_2PO_4 and glycerol-phosphate were run alongside samples and used to calculate digestion efficiency (~87.5%) which was used to correct TP estimates. Samples were digested for 55 min at 121 °C in an autoclave, then cooled subsamples were used for determination of SRP, with absorbance read at 850 nm in a microtiter plate (Molecular Devices, Sunnyvale, CA, USA). TP measurements were averaged and used as N_T for the model.

Bacteria and virus abundances

Samples were collected daily for determination of bacteria and virus abundances. Bacteria and viruses were enumerated by epifluorescence microscopy (Noble and Fuhrman, 1998). 1 mL samples were vacuum filtered onto a 0.2 μm 25 mm Anodisc filter (Whatman, Maidstone, Kent, UK). Filters were stained with 100 μL of SYBR® Green (Molecular Probes, Eugene, OR, USA) at 1:400 dilution for 12–15 min. Filters were placed on individual glass slides and 30 μL of antifade mounting solution (Noble and Fuhrman, 1998) was applied to each filter. The samples were observed under an Olympus BX41 microscope with a mercury lamp and DAPI epifluorescence filter set (excitation 330–385 nm, 400 nm dichroic mirror and long pass emission >420 nm) using oil immersion at 100× objective and an ocular grid (100 squares, each representing an area of 10^{-4} mm^2). Grid squares were randomly chosen and viruses or bacteria were counted until a total of >200 viruses or bacteria was reached (typically >10 different fields of view). Abundance was calculated based on the number of squares counted and volume filtered.

Determination of chl a fluorescence and chlorophyll concentrations

In order to monitor phytoplankton biomass in samples, chlorophyll (chl) *a* fluorescence was measured in water samples collected from day 2 to 14 using a TD700 fluorometer (equipped with an in vitro filter set and a red-sensitive photomultiplier tube, Turner Designs, Sunnyvale, CA, USA), using distilled, deionized water as a blank. On selected days chl *a* concentration was measured. Replicate 500 mL samples were vacuum filtered onto 25 mm A/E filters (Pall Life Sciences, Ann Arbor, MI, USA), extracted in 90% acetone overnight at −20 °C and chl *a* measured using a spectrophotometric method, correcting for phaeopigments (Parsons et al., 1984).

Statistical analyses

Statistical analyses to examine changes in measured variables over time in enriched and control carboys were carried out using SigmaStat version V. 3.1 (Systat Software Inc., Chicago, USA). Linear regression was performed for each variable against time, and the significance of the regression (i.e. whether the slope differed from zero) was tested at the 95% confidence level (i.e. probability of a Type I error set at 0.05).

Model parameter estimation

Viral and bacterial abundances were used to estimate parameters of the model (see Fig. 1), optimizing the fit separately for each carboy. Data were smoothed using two-day running averages of the experimental

data. The fitting constituted an inverse problem. Model differential equations were solved using the ode23s solver in MATLAB (The Mathworks Inc., Natick, MA, USA), which is based on a modified Rosenbrock formula of order 2 (Shampine and Reichelt, 1997). The parameter estimation was done using the *fminsearch* function in MATLAB, employing the Nelder–Mead algorithm (Olsson and Nelson, 1975). The model was initially calibrated with fixed parameters based on literature values (Table 1), or experimental measurements. The estimated parameters were burst size (b) and latent period ($1/\lambda$) and a measure of viral persistence, the viral decay rate (d). Both burst size and latent period are known to vary with nutrient status in aquatic ecosystems or experiments (e.g. Jacquet et al., 2002; Parada et al., 2006) and viral decay rate has not been estimated for Lake Michigan. Importantly, when running the model, estimated parameters were constrained to those which were deemed biologically reasonable by introducing penalties to the model's cost function. For example, although burst size can vary considerably (Parada et al., 2006), negative values clearly have no meaning, thus heavy penalties were imposed for such unreal values. Model fit was assessed using relative error: (observed value − estimated value) / observed value (see Dym, 2004). Relative error was calculated separately for bacterial and viral abundances; the modeling minimized the sum of the two.

Our preliminary work showed that algae present in the cultures, but not prone to lysis, took up free nutrients. Therefore, it was necessary to add an algal component, A, representing nutrient uptake by algae (phytoplankton) to the Fuhrman et al. (2011) model. The additional basic equations used in the new model were:

$$dA/dt = \mu_A(Q_A)A \tag{7}$$

$$dQ_A/dt = \rho_A(N,Q) - \mu_A(Q_A)Q_A \tag{8}$$

And new essential equations that then linked algal biomass and growth to free nutrient concentration were:

$$\mu(Q_A) = \mu_{\max\,algae}\left(1 - Q_{\min\,algae}/Q_A\right) \tag{9}$$

$$\rho_A(N,Q_A) \equiv \rho_A(N) = \rho_{max\,algae} N\left(K_{n\,algae} + N\right)^{-1} \tag{10}$$

where and $\mu(Q_A)$ is a growth function which follows Michaelis–Menten kinetics and $\rho_A(N,Q)$ is a nutrient uptake function which follows a Monod kinetic, as for Eqs. (5) and (6), but for algae. For the experimental period, there was no evidence of algal mortality or subsequent nutrient release. Therefore, terms for these processes were not included and algae represented essentially a sink for nutrients. Free nutrient (N) was not modeled independently, but was calculated at each time step by subtracting nutrient contained in bacteria, viruses and algae (i.e. product of content and abundance) from total nutrient (N_T).

Results

Although they were treated similarly, replicate carboys behaved differently and had unique nutrient, bacterial and viral abundance datasets. As such, data were modeled and presented separately for each carboy.

Bacteria and virus populations

Bacterial abundance varied over the 14 days in both control and enriched cultures (range 2.53–5.38 × 10^9 cells/L, Fig. 2), but did not significantly increase or decrease over the experiment (linear regression of bacterial abundance against time, $P > 0.09$ in all cases). Virus abundance also fluctuated in all cultures over the 14 days (Fig. 2). For unenriched control samples, viruses ranged from 1.9 to 3.7 × 10^{10} viruses/L, with no consistent change over time (linear regression of viral particle abundance against time, $P > 0.2$ in both cases). For P enriched carboys, virus abundance ranged from 1.3 to 3.9 × 10^{10} viruses/L and significantly increased over time (linear regression of viral abundance against time, $P < 0.05$ in both cases).

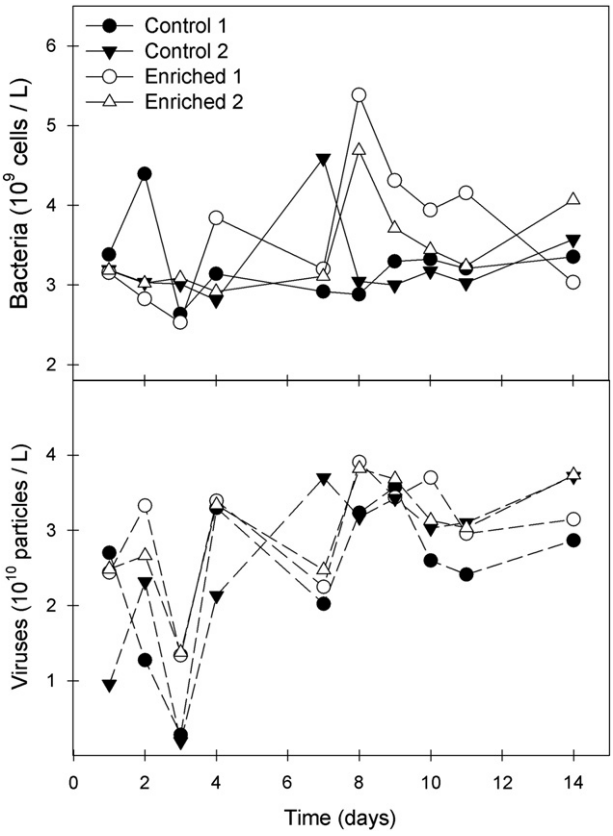

Fig. 2. Bacterial and virus abundances in Lake Michigan measured in samples collected from control and phosphorus-enriched carboys over 14 days.

Phytoplankton biomass

Changes in chl *a* fluorescence were not consistent among carboys (Fig. 3). The control 2 culture showed no changes in chl *a* (linear regression of chl *a* fluorescence against time, $P > 0.2$), but the other three carboys showed transient increases over the first 4 days then declined to near initial levels (Fig. 3). Chl *a* fluorescence data correlated well

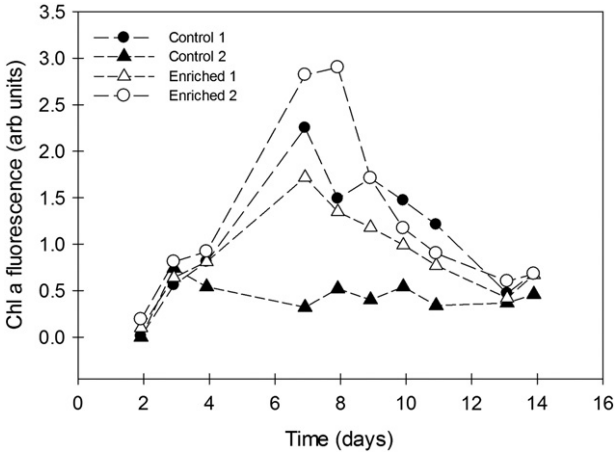

Fig. 3. Chlorophyll *a* fluorescence as a measure of phytoplankton biomass in Lake Michigan samples collected from control and P enriched carboys over 14 days.

with extracted chl within treatments, but varied between control and P enriched treatments; markedly higher ratios of fluorescence/chl *a* were found for P enriched versus control carboys (580 vs. 166 fluorescence units/μg/L chl *a* respectively) (data not shown).

Phosphorus pools

The measured SRP in the unenriched control carboys remained very low and stable for the duration of the experiment (linear regression of SRP over time, $P > 0.2$ in both cases) and was often below detection limit (~0.05 μM, using a 10 cm cuvette) (Fig. 4). In P enriched samples, SRP declined from initial enrichment levels (7.5–8 μM) to below 6 μM over the 14 days (linear regression of SRP over time, $P < 0.002$ in both cases) (Fig. 4). Total P (TP) in all carboys did not change over time (linear regression of TP over time, $P > 0.1$ in all cases) indicating a closed internal P budget. There was ~8 μM TP in P enriched treatments and <0.5 μM in control treatments (data not shown).

Model simulation

Model estimates of the host–virus parameters, burst size, virus decay rate and latent period along with relative errors of these estimates are in Table 2. There were clear differences in burst size with control carboys having two to three times the burst size estimated for P enriched carboys and estimates for replicate carboys in each treatment were relatively close (Table 2). Estimates of the latent period ($1/\lambda$) were shorter in P enriched than control carboys, but viral decay rates (d) were more similar between the four carboys. The model fits to the

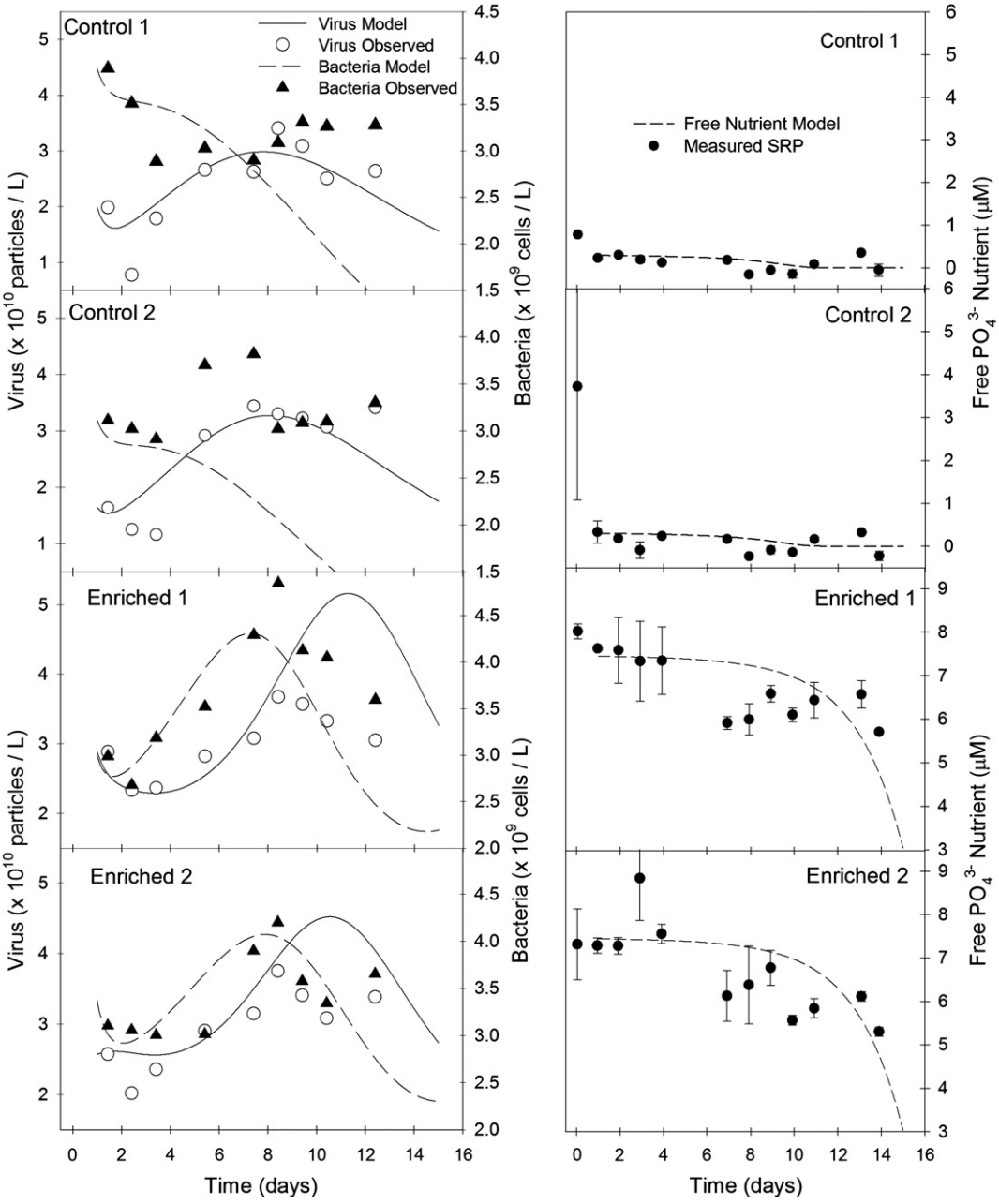

Fig. 4. Model fit with optimized parameters for four carboys, with two untreated control carboys (top two) and two phosphorus-enriched carboys (lower two). Left panels show bacteria and virus data (symbols) and models (lines) for each carboy, with each data point representing a two-day running average of the measured values (in Fig. 2). Right panels show free PO_4^{3-} nutrient concentration as measured SRP values (symbols) and modeled free nutrient concentration (dotted line); points are means of triplicate water samples collected and analyzed at each time point, error is standard deviation. See Table 1 for model parameters and Table 2 for numerical results of parameter estimation.

Table 2
Optimized parameters derived from the model and relative error of modeled predictions to experimental data.

Treatment replicate	Burst size b	Latent period 1/λ (d)	Virus decay rate d (/d)	Relative error (bacteria)	Relative error (virus)
Control 1	188	6.25	1.70	0.130	0.110
Control 2	192	6.67	1.37	0.238	0.087
P enriched 1	55.2	1.37	1.20	0.0444	0.117
P enriched 2	64.6	1.04	1.40	0.0520	0.144

experimental data in P enriched carboys were qualitatively good showing similar virus–host dynamics between the two replicate carboys over the 14 days (Fig. 4). The model fits for the unenriched controls showed less clear pattern of host–virus changes between replicate carboys (Fig. 4). The model fits to bacterial abundance were particularly poor in the control carboys, reflected in the much higher relative error associated with estimates for bacteria (Table 2).

Discussion

The differences in fitting of the host–virus interaction model incorporating cell nutrient status with experimental data from natural P limited versus P enriched samples demonstrate that nutrient status is important in how well such models can predict host–virus dynamics in freshwater ecosystems, and emphasize the importance of nutrients in host–virus interactions (Scanlan and Wilson, 1999). In many freshwater ecosystems, including Lake Michigan and the upper Great Lakes, primary production is typically limited by chronically low P availability (Schelske et al., 1974; Schindler, 1977). This was the case in the control treatments where P limitation clearly affected phytoplankton growth and virus–host dynamics. The stimulation of phytoplankton production, observed as generally higher chl *a* fluorescence in P enriched carboys (at least before day 10), contrasted with a lack of stimulation of bacterial abundance. This suggests that, while primary production was limited by P, bacteria responded to other factors that increased later in cultures, possibly organic C supply (cf. Cotner and Wetzel, 1992). Alternatively, bacterial abundance may have increased, but they were 'cropped' via lysis resulting from viral infection; evidence for this was the increases in free virus abundance (Fig. 2), which could presumably only have resulted from infected host cells releasing free virus.

The model simulations for the P enriched carboys followed the oscillating host bacteria–virus dynamics captured by other models (e.g., Beretta and Kuang, 1998; Gons et al., 2006; Middelboe, 2000; Rodriguez-Brito et al., 2010) (Fig. 4), with good fits of the model to observed parameters. However, the model simulations using the optimized parameters for the unenriched control treatment were not as successful, particularly for estimating bacterial abundance which had much higher error for model estimates in control than P enriched carboys (Table 2). This discrepancy in model fits between enriched and control carboy data suggests that assumptions about host–virus interactions and P fluxes, which are accurate or tolerated by the model under nutrient replete conditions, are not accurate under P limiting conditions. Thus, the current model is likely to be most useful in meso- to eutrophic systems. The host–virus model used as the basis for the development of the Fuhrman et al. (2011) model was based on single host–single virus interactions in nutrient-replete conditions (e.g., Gons et al., 2006). Nutrient limitation, along with greater complexity of host cell and virus interactions in natural waters, could provide additional modeling challenges. The discrepancy in model accuracy in predicting virus-bacterial populations between P replete and limiting conditions could relate to P availability for cell growth, energy production and virus replication.

Another factor to consider is grazing. Screening to remove nanograzers has been used (Bouvy et al., 2011), but our preliminary work with 5 μm or 1 μm Nitex screens gave either poor grazer removal or resulted in substantial removal of bacteria, so we have no clear means to estimate their effects on bacteria or viruses. Data for grazing on autotrophs from size-fractionated dilution experiments conducted at the Fox Point station at the same time of year in previous years (Sandgren and Berges, unpublished), suggest very low rates. Significant grazing occurred only in the <10 μm fraction and represented just 0.001 μg chl/L/d. Assuming comparable grazing in our incubations, this would represent less than 1% of the chl *a* over 14 days and is consistent with the very small changes observed in control carboys. Given the large volumes used, it is difficult to see why nanograzers would differ among carboys, thus this is unlikely to explain differences among replicates. In contrast, Bouvy et al. (2011) demonstrated marked depletion of algae, bacteria and viruses due to nanograzers. One reason for the difference might be trophic status; Bouvy et al. worked in a Mediterranean lagoon system with substantially higher biomass.

Model-estimated parameters

The estimates of unknown virus–host parameters derived by the model showed clear differences between control and P enriched carboys for burst size and latent period (Table 2). Replicate parameter estimates for the two carboys for each treatment were relatively close, and the model optimization routine derived parameter estimates in the range reported in the literature from empirical measurements in samples from aquatic ecosystems.

Burst size

Model estimates of burst size ranging from 55 to 192 are similar to 4–140 reported for oligotrophic–mesotrophic freshwaters (reviewed by Parada et al., 2006) and 21–121 for mesotrophic Lake Constance (Hennes and Simon, 1995). Across ecosystems, there is little consistent effect of nutrient status on burst size, however burst size is reportedly extremely low (2–15) in oligotrophic arctic waters (Säwström et al., 2007) compared with 16–70 in mesotrophic–hypertrophic lakes (Liu et al., 2006). Within experimental studies, there is some evidence that lower burst size is associated with more nutrient limiting conditions (Bratbak et al., 1998; Jacquet et al., 2002) and cells in low growth rate or stationary phase show reduced burst size compared to cells growing in exponential phase (Bratbak et al., 1998; Middelboe, 2000). In contrast, the model estimates for burst size in P limited control carboys of Lake Michigan water were higher than in P enriched conditions. Given the high P demand for nucleic acid synthesis, one might expect P limitation to limit virus reproduction (Wilson et al., 1996). Typically, as bacterial production increases, burst size goes up (Middelboe, 2000), however there was little evidence for increases in net bacterial growth in the P enriched carboys. Modeling of an algal-virus system suggested that increased viral lysis of algal host *Phaeocystis pouchetii* released enough P to help alleviate P limitation for the algal cells in enclosed culture conditions (Thyrhaug et al., 2003). If bacterial host cell lysis rates were higher in control carboys, and P turnover rates were higher, then this may have improved P availability for higher virus replication prior to host lysis.

Latent period

The latent period range, 1.04–6.67 days, was higher than the ranges generally reported from other experimental and modeled host–virus systems; Bratbak et al. (1998) and Thyrhaug et al. (2003) both used 15 h and Gons et al. (2006) used 12 h in models and even lower latent periods (1–2 h) have been reported for cultured host–virus systems (Middelboe, 2000). In the previous model, Fuhrman et al. (2011) used a latent period of 5 days. The two control carboys which had higher burst size also had longer latent periods, suggesting that the replication of more virus particles in each host cell results in delayed lysis. Lower availability of P to support replication of viral nucleic acids could also

increase latent period in the control carboys (Wilson et al., 1996). In chemostat-grown bacteria, increasing nutrient limitation resulted in longer latent periods, however this was accompanied by decreased burst size (Middelboe, 2000). It is unclear how to reconcile model estimates of increased latent period along with increased burst size in P limited carboys, but higher P turnover rates from host cells might contribute to these findings.

Virus decay rate

The virus decay rate was fairly similar in all carboys, between 1.2 and 1.7/d, mostly within the range reported in the literature; 0.5/d used by Gons et al. (2006), 0.12/d empirically determined for a freshwater lake (Thomas et al., 2011) and 0.96–1.6/d for some marine viruses (Noble and Fuhrman, 1997). However, other experimentally determined rates in freshwater are much higher (7–14/d, Heldal and Bratbak, 1991). Virus decay rates include grazing and in natural waters can be hastened by UV radiation and dissolved and particulate material in the water (Liu et al., 2011; Noble and Fuhrman, 1997). Although UV would not have been a significant factor in our indoor laboratory incubations, dissolved and particulate substances were not examined.

New contributions and limitations of the model

The modified model presented and tested in this study incorporated free nutrient (P) uptake by phytoplankton (algae), whereas this was not a component of previous host–virus models (e.g. Fuhrman et al., 2011; Gons et al., 2006). Despite lack of clear bacterial growth stimulation with P addition (Fig. 2), drawdown of SRP was observed, although the model appeared to overestimate drawdown near the end of the 14 day experiment (Fig. 4). Uptake by phytoplankton would result in a change in P status of phytoplankton cells in P enriched carboys relative to controls, and indeed, fluorescence per unit chl was higher for P enriched versus control carboys by the end of the experiment. Increased fluorescence output per chl has been related to alleviation of P limitation in phytoplankton (Geider et al., 1993). Incorporation of phytoplankton P uptake into the nutrient-based model of host–virus interactions demonstrates the adaptability of this host–virus nutrient model.

Phosphorus limitation

The model estimates and qualitative fits to the data suggest that different model versions may be needed to accurately model nutrient limited vs. nutrient replete conditions. One possible reason for the differences between control and P enriched carboys is the expectation that burst size should be lower when P is more limited, in the control carboys. While P was clearly in much lower supply in control carboys, but in vast excess in the P enriched carboys, there was also very low biomass in the Lake Michigan water, and the natural phytoplankton and bacterial populations are well adapted to chronic P limitation in Lake Michigan waters (Young et al., 2010). P availability was assessed as concentrations within the carboys, using filtered subsamples withdrawn regularly from carboys and assayed using methods with detection limits of ~50 nM. However, phytoplankton and planktonic bacteria have high uptake affinity for phosphate, with estimates of half saturation constants for phosphate uptake ~5 nM for algae (Jansson, 1993) and ~10 nM for bacteria (Thingstad et al., 1993). Additionally, viral lysis of host cells releases P to the nutrient pool (Fig. 1) (Gobler et al., 1997), so high lysis rates could release P supply on rapid time scales and small spatial scales not well captured by measurements of static P concentrations (Moutin et al., 2002; Thingstad et al., 1993). The model assumes that P released from viral lysis is completely and instantly available. Although this assumption is unrealistic, abundant activity of extracellular alkaline phosphatase (Rengefors et al., 2003; Young et al., 2010) would broaden access from just orthophosphate to include some organic P sources. Therefore, even in control carboys, there may have been enough P available for bacterial uptake and use in viral replication and biomass production may not have been as extremely P limited in the control carboys as expected. This could drive higher burst size in control carboys despite host–virus dynamics being clearly different under low P supply to when free P is in vast excess (P enriched carboys).

Another key factor in P acquisition by chronically P limited cells such as Lake Michigan phytoplankton, is viral phosphate transporters. In P limited oligotrophic areas of the ocean, there is evidence for genes encoding high affinity phosphate transporters in viral genomes, which may help mitigate P starvation by increasing host cell affinity for scarce phosphate (Kelly et al., 2013; Monier et al., 2012). Chronic P limitation in oligotrophic lakes could provide similar selection criteria for viruses carrying genes involved in P acquisition. If infecting viruses carry genes which stimulate host cell P uptake, incorporation and expression of these genes resulting in up-regulated de novo synthesis of host cell transporters would take some time, so one might expect the latent period to increase, as was observed in control carboys compared with P replete treatments. It would also follow that if infected cells have higher P uptake and more intracellular P resources available to produce new virus particles, then a larger burst size might also result, as observed in the control carboys. Such a trade-off between larger burst size and longer latent period, possibly aided by viral up-regulation of host P acquisition vs. shorter latent period and smaller burst size when P is in excess supply, could reflect different virus infection strategies in response to nutrient limitation (Monier et al., 2012). The prevalence or significance of viral nutrient transporter genes in freshwaters is completely unknown, though ongoing metagenomics projects in the Great Lakes might yield some important insights.

Lytic and lysogenic viral infection

A documented response of host–virus interactions and viral behavior in oligotrophic conditions, particularly under P limitation, is to induce the lysogenic phase (Scanlan and Wilson, 1999). This has been associated with particularly low bacterial production rates in freshwaters (Thomas et al., 2011) and suggested for oligotrophic Lake Superior (Tapper and Hicks, 1998); evidence for lysogenic virus behavior in natural systems comes from lateral gene transfer from host to virus (e.g. Monier et al., 2012). Currently the model developed by Fuhrman et al. (2011) and tested in this study specifically addresses only lytic virus infection. However, considering the chronic nutrient (P) limitation stress on the bacterial populations in many freshwater lakes, a portion of viruses may be in the lysogenic phase (Scanlan and Wilson, 1999). Lysogenic infection does not involve regular host release of new virus particles so estimation of free virus particles would not address lysogenic infection. Although precise environmental triggers driving lysogenic vs. lytic viral infection are still not clear (Wilson and Mann, 1997), and balance between lysogeny and lytic infection was not assessed, there was no clear evidence for lower virus counts in P limited carboys than P enriched, suggesting that there was no *large* diversion from lytic to lysogenic infection in control carboys. However, estimation of lysogenic vs. lytic virus infections should be incorporated into future developments of the model. As part of estimating lysogenic vs. lytic phases, empirical measurement of virus burst size (e.g. Bratbak et al., 1998) would also be important and help verify model estimates.

Host cell viability

A possible source of error in empirical estimates of virus and bacterial abundance is that quantification relied on SYBR® Gold staining which binds to all genetic material present in the sample, providing a fluorescent signal for both living and dead cells. If there were appreciably higher number of dead cells within the control treatments (see Schumann et al., 2003), the experimental cell abundances used to parameterize the model may have been inflated, leading to increased errors in model estimates of bacterial abundance (Table 2). Estimation

of the proportions of living vs. dead cells using mortal staining such as SYTOX® (Schumann et al., 2003), using microscopy or in conjunction with flow cytometry would also provide more accurate input host cell parameters for the model. Further testing of the model using these additional parameters and components should focus on comparisons of samples across the trophic spectrum (i.e. oligotrophic–eutrophic freshwater ecosystems) to further examine roles of nutrient limitation in how well models predicts natural host–virus dynamics.

Conclusions for future model development

The recent Fuhrman et al. (2011) model incorporates a nutrient cell quota and nutrient uptake important to understanding the role of viruses in nutrient cycling in aquatic ecosystems, which we have further developed by incorporating nutrient uptake by phytoplankton. Testing the model against experimental measurements for Lake Michigan demonstrated that the model works well for predicting virus–host population dynamics in P replete conditions, but less well under P limitation. This suggests that application of the virus–host model to chronically P limiting conditions may not be incorporating all essential variables, or some assumptions about the function of the host–virus interaction under P limitation are not accurate. As P availability is critically important to viral replication (Monier et al., 2012; Wilson and Mann, 1997; Wilson et al., 1996), and P stress may be an important factor in virus selection (Kelly et al., 2013), P limited freshwater lakes provide excellent systems to refine virus–host-nutrient models in conjunction with empirical measurements. In order to develop and refine the model for application to chronically P limited freshwater ecosystems, additional parameters need to be assessed to parameterize and test the model. Some key variables which need to be empirically determined include live/dead host cell proportions, uptake kinetics of dissolved organic P forms as well as phosphate, proportions of lysogenic vs. lytic virus infection under nutrient limitation or replete conditions, and any role of virus P transporter genes in host cell nutrient responses. Differences in marine versus freshwater ecosystems in terms of the role of viruses in nutrient-driven host–virus dynamics (Clasen et al., 2008; Wilhelm and Matteson, 2008), could also be examined using this model.

Acknowledgments

We thank the captain and crew of the *R/V Neeskay* and personnel at the School of Freshwater Sciences for help with sample collection. AB, TS and MT were participants in the UWM Undergraduate Research in Aquatic Biology and Mathematics (UBM) program, funded, in part, by National Science Foundation under a UBM-Group Award 082717.

References

Beretta, E., Kuang, Y., 1998. Modeling and analysis of a marine bacteriophage infection. Math. Biosci. 149, 57–76.
Bouvy, M., Bettarel, Y., Bouvier, C., et al., 2011. Trophic interactions between viruses, bacteria and nanoflagellates under various nutrient conditions and simulated climate change. Environ. Microbiol. 13, 1842–1857.
Bratbak, G., Jacobsen, A., Heldal, M., 1998. Viral lysis of *Phaeocystis pouchetii* and bacterial secondary production. Aquat. Microb. Ecol. 16, 11–16.
Clasen, J.L., Brigden, S.M., Payet, J.P., Suttle, C.A., 2008. Evidence that viral abundance across oceans and lakes is driven by different biological factors. Freshw. Biol. 53, 1090–1100.
Cotner, J.B., Wetzel, R.G., 1992. Uptake of dissolved inorganic and organic phosphorus compounds by phytoplankton and bacterioplankton. Limnol. Oceanogr. 37, 232–243.
Cunningham, A., Nisbet, R., 1983. Transient oscillation in continuous culture (chapter 3). In: Bazin, M. (Ed.), Mathematics and Microbiology. Academic Press, London, pp. 77–103.
DeBruyn, J.M., Leigh-Bell, J.A., McKay, R.M.L., Bourbonniere, R.A., Wilhelm, S.W., 2004. Microbial distributions and the impact of phosphorus on bacterial activity in Lake Erie. J. Great Lakes Res. 30, 18–166.
Droop, M.R., 1974. The nutrient status of algal cells in continuous culture. J. Mar. Biol. Assoc. U. K. 54, 825–855.
Dym, C.L., 2004. Principles of Mathematical Modeling, Second edition. Elsevier Academic Press.
Fu, F., Zhang, Y., Bell, P., Hutchins, D., 2005. Phosphate uptake and growth kinetics of *Trichodesmium* (cyanobacteria) isolates from the North Atlantic Ocean and the Great Barrier Reef, Australia. J. Phycol. 41, 62–73.
Fuhrman, J., 1999. Marine viruses and their biogeochemical and ecological consequences. Nature 399, 541–548.
Fuhrman, K.M., Pinter, G.A., Berges, J.A., 2011. Dynamics of a virus–host model with an intrinsic quota. Math. Comput. Model. 53, 716–730.
Gastrich, M.D., Leigh-Bell, J.A., Gobler, C.J., Anderson, O.R., Wilhelm, S.W., Bryan, M., 2004. Viruses as potential regulators of regional brown tide blooms caused by the alga, *Aureococcus anophagefferens*. Estuarine 27, 112–119.
Geider, R.J., LaRoche, J., Greene, R.M., Olaizola, M., 1993. Response of the photosynthetic apparatus of *Phaeodactylum tricornutum* (Bacillariophyceae) to nitrate, phosphate, or iron starvation. J. Phycol. 29, 755–766.
Gobler, C.J., Hutchins, D.A., Fisher, N.S., Cosper, E.M., Sanudo-Wilhelmy, S.A., 1997. Release and bioavailability of C, N, P, Se, and Fe following viral lysis of a marine chrysophyte. Limnol. Oceanogr. 42, 1492–1504.
Gons, H.J., 1995. Interaction of detritus with abundance of cyanobacteria and microalgae. Water Sci. Technol. 32, 129–138.
Gons, H.J., Hoogveld, H.L., Simis, S.G.H., Tijdens, M., 2006. Dynamic modeling of viral impact on cyanobacterial populations in shallow lakes: implications of burst size. J. Mar. Biol. Assoc. U.K. 86, 537–542.
Heldal, M., Bratbak, G., 1991. Production and decay of viruses in aquatic environments. Mar. Ecol. Prog. Ser. 72, 205–212.
Hennes, K.P., Simon, M., 1995. Significance of bacteriophages for controlling bacterioplankton growth in a mesotrophic lake. Appl. Environ. Microbiol. 61, 333–340.
Jacquet, S., Heldal, M., Iglesias-Rodriguez, D., Larsen, A., Wilson, W., Bratbak, G., 2002. Flow cytometric analysis of an *Emiliana huxleyi* bloom terminated by viral infection. Aquat. Microb. Ecol. 27, 111–124.
Jacquet, S., Miki, T., Noble, R., Peduzzi, P., Wilhelm, S., 2010. Viruses in aquatic ecosystems: important advancements of the last 20 years and prospects for the future in the field of microbial oceanography and limnology. Adv. Oceanogr. Limnol. 1, 97–141.
Jansson, M., 1993. Uptake, exchange, and excretion of orthophosphate in phosphate-starved *Scenedesmus quadricauda* and *Pseudomonas* k7. Limnol. Oceanogr. 38, 1162–1178.
Kelly, L., Ding, H., Huang, K.H., Osburne, M.S., Chisholm, S.W., 2013. Genetic diversity in cultured and wild marine cyanomyoviruses reveals phosphorus stress as a strong selective agent. ISME J. 7, 1827–1841.
Liu, Y.M., Zhang, Q.Y., Yuan, X.P., Li, Z.Q., Gui, J.F., 2006. Seasonal variation of virioplankton in a eutrophic shallow lake. Hydrobiology 560, 323–334.
Liu, W., Cheng, K., Zhao, Y.J., Wu, Y.J., Cai, C.F., Lu, S.Y., Jin, X.C., 2011. Cyanophage decay and its causes in eutrophic freshwater. J. Food Agric. Environ. 9, 963–966.
Menzel, D.W., Corwin, N., 1965. The measurement of total phosphorus in seawater based on the liberation of organically bound fractions by persulfate oxidation. Limnol. Oceanogr. 10, 280–282.
Middelboe, M., 2000. Bacterial growth rate and marine virus–host dynamics. Microb. Ecol. 40, 114–124.
Middelboe, M., Jacquet, S., Weinbauer, M., 2008. Viruses in freshwater ecosystems: an introduction to the exploration of viruses in new aquatic habitats. Freshw. Biol. 53, 1069–1075.
Monier, A., Welsh, R.M., Gentemann, C., Weinstock, G., Sodergren, E., Armbrust, E.V., Eisen, J.A., Worden, A.Z., 2012. Phosphate transporters in marine phytoplankton and their viruses: cross-domain commonalities in viral–host gene exchanges. Environ. Microbiol. 14, 162–176.
Moutin, T., Thingstad, T.F., Van Wambeke, F., Marie, D., Slawyk, G., Raimbault, P., Claustre, H., 2002. Does competition for nanomolar phosphate supply explain the predominance of the cyanobacterium *Synechococcus*? Limnol. Oceanogr. 47, 1562–1567.
Murray, A.G., Jackson, G.A., 1992. Viral dynamics: a model of the effects of size, shape, motion and abundance of single-celled planktonic organisms and other particles. Mar. Ecol. Prog. Ser. 89, 103–116.
Noble, R.T., Fuhrman, J.A., 1997. Virus decay and its causes in coastal waters. Appl. Environ. Microbiol. 63 (1), 77–83.
Noble, R.T., Fuhrman, J.A., 1998. Use of SYBR Green I for rapid epifluorescence counts of marine viruses and bacteria. Aquat. Microb. Ecol. 14, 113–118.
Olsson, D.M., Nelson, L.S., 1975. The Nelder–Mead simplex procedure for function minimization. Technometics 17, 45–51.
Parada, V., Herndl, G.J., Weinbauer, M.G., 2006. Viral burst size of heterotrophic prokaryotes in aquatic systems. J. Mar. Biol. Assoc. U.K. 86, 613–621.
Parsons, T.R., Maita, Y., Lalli, C.M., 1984. A Manual of Chemical and Biological Methods for Seawater Analysis. Pergamon Press, Elmsford.
Poorvin, L., Rinta-Kanto, J.M., Hutchins, D.A., Wilhelm, S.W., 2004. Viral release of iron and its bioavailability to marine plankton. Limnol. Oceanogr. 49, 1734–1741.
Rengefors, K., Ruttenberg, K.C., Haupert, C.L., Taylor, C., Howes, B.L., Anderson, D.M., 2003. Experimental investigation of taxon-specific response of alkaline phosphatase activity in natural freshwater phytoplankton. Limnol. Oceanogr. 48, 1167–1175.
Rodriguez-Brito, B., Li, L.L., Wegley, L., et al., 2010. Viral and microbial community dynamics in four aquatic environments. ISME J. 4, 739–751.
Säwström, C., Graneli, W., Laybourn-Parry, J., Anesio, A.M., 2007. High viral infection rates in Antarctic and Arctic bacterioplankton. Environ. Microbiol. 9, 250–255.
Scanlan, D.J., Wilson, W.H., 1999. Application of molecular techniques to addressing the role of P as a key effector in marine systems. Hydrobiology 401, 149–175.
Schelske, C.L., Rothman, E.D., Stoermer, E.F., Santiago, M.A., 1974. Responses of phosphorus limited Lake Michigan phytoplankton to factorial enrichments with nitrogen and phosphorus. Limnol. Oceanogr. 19, 409–419.
Schindler, D.W., 1977. Evaluation of phosphorus limitation in lakes. Science 195, 260–262.
Schumann, R., Schiewer, U., Karsten, U., Rieling, T., 2003. Viability of bacteria from different aquatic habitats. II. Cellular fluorescent markers for membrane integrity and metabolic activity. Aquat. Microb. Ecol. 32, 137–150.

Shampine, L.F., Reichelt, M.W., 1997. The MATLAB ode suite. SIAM J. Sci. Comput. 18, 1–22.
Smith, R.E., Kalff, J., 1982. Size-dependent phosphorus uptake kinetics and cell quota in phytoplankton. J. Phycol. 18, 275–284.
Tapper, M.A., Hicks, R.E., 1998. Temperate viruses and lysogeny in Lake Superior bacterioplankton. Limnol. Oceanogr. 43, 95–103.
Thingstad, T.F., Skjoldal, E.F., Bohne, R.A., 1993. Phosphorus cycling and algal-bacterial competition in Sandsfjord, western Norway. Mar. Ecol. Prog. Ser. 99, 239–259.
Thomas, R., Berdjeb, L., Sime-Ngando, T., Lyria, B., Telesphore, S.-N., Jacquet, S., 2011. Viral abundance, production, decay rates and life strategies (lysogeny versus lysis) in Lake Bourget (France). Environ. Microbiol. 3, 616–630.
Thyrhaug, R., Larsen, A., Thingstad, T.F., Bratbak, G., 2003. Stable coexistence in marine algal host–virus systems. Mar. Ecol. Prog. Ser. 254, 27–35.
Weinbauer, M.G., Chen, F., Wilhelm, S.W., 2011. Virus-mediated redistribution and partitioning of carbon in the global oceans. In: Jiao, N., Azam, F., Sanders, S. (Eds.), Microbial Carbon Pump in the Ocean. Science/AAAS, Washington, DC, pp. 54–56.
Wilhelm, S.W., Matteson, A.R., 2008. Freshwater and marine virioplankton: a brief overview of commonalities and differences. Freshw. Biol. 53, 1076–1089.
Wilson, W.H., Mann, N.H., 1997. Lysogenic and lytic production in marine microbial communities. Aquat. Microb. Ecol. 13, 95–100.
Wilson, W.H., Carr, N.G., Mann, N.H., 1996. The effect of phosphate status on the kinetics of cyanophage infection in the oceanic cyanobacterium *Synechococcus* sp. WH7803. J. Phycol. 32, 506–516.
Young, E.B., Tucker, R.C., Pansch, L., 2010. Alkaline phosphatase in freshwater *Cladophora*-epiphyte assemblages: regulation in response to phosphorus supply and localization. J. Phycol. 46, 93–101.